AN ASSESSMENT OF METHODS FOR ESTIMATING RUNOFF RATES AT THE PLOT SCALE

B. Yu, U. Cakurs, C. W. Rose

ABSTRACT. *As distinct from the USLE/RULSE for which only rainfall rate is required to quantify the climatic influence on soil erosion, information on runoff rate in addition to rainfall rate is needed to drive all the process-based soil erosion models. For numerous runoff and soil loss plots around the world, only event-based runoff amounts have been measured regularly. To estimate soil erodibility parameters for these process-based soil erosion models and to facilitate their use, methods for estimating the runoff rate for given runoff amount are clearly needed. Three one-parameter infiltration models were examined, and estimated and observed runoff rates were compared for six bare plots in the tropical and subtropical regions of Southeast Asia and Australia. The model which characterizes the spatial variability in the maximum rate of infiltration performed best in comparison with other models assuming either a constant or a proportional infiltration rate. The spatially variable infiltration model has little bias in estimated runoff rate and works equally well for data collected at different time intervals. At a typical time interval of 6 min, the relative bias of the estimated peak runoff rate is 6% and the mean absolute error is 4.6 mm/h. The ratio of root mean square error to peak runoff rate was found to decrease as the runoff coefficient increases.*

Keywords. *Infiltration, Erosion, Soil erosion models, Australia, Southeast Asia.*

Globally nearly two billion hectares, or about 13% of the Earth's land surface, have suffered some type of human-induced land degradation (Oldeman et al., 1991), and water erosion has been the main cause of this land degradation. For soil conservation planning and erosion impact assessment, the Universal Soil Loss Equation (USLE) (Wischmeier and Smith, 1978) and more recently RUSLE (Renard et al., 1997) have been widely used to predict long-term average soil loss from agricultural lands. In recent years, process-based erosion models, such as WEPP (Water Erosion Prediction Project) (Lane and Nearing, 1995; Laflen et al., 1991b) and GUEST (Griffith University Erosion System Template) (Misra and Rose, 1996), among others, were developed for soil loss predictions. Potential advantages of using these later erosion models include involvement of physically meaningful erodibility parameters, and unlike the K-factor in the USLE/RUSLE determination of these parameters does not require long-term monitoring of soil losses from bare fallow plots.

As distinct from the USLE/RUSLE, hydrologic variables such as runoff rate and total runoff depth are explicitly required to drive these process-based erosion models for soil loss predictions. In WEPP, for example, both detachment and transport capacities are related to the peak runoff rate, q_p, via hydraulic shear stress (Foster et al., 1995), and the runoff depth is needed to compute an effective runoff duration. In GUEST, sediment concentration is related to the stream power which in turn depends on the runoff rate (Misra and Rose, 1996). For a storm event, the flow-weighted average sediment concentration is related to an effective runoff rate (Rose, 1994; Ciesiolka et al., 1995a), q_e, defined as:

$$q_e = \left(\frac{\sum q_i^{1.4}}{\sum q_i} \right)^{2.5} \quad (1)$$

where q_i is the runoff rate for the time interval i, and the summation applies for the duration of the runoff event. The product of runoff depth and the average sediment concentration will then give the amount of soil loss per unit area for the event. Both the peak runoff rate and the effective runoff rate in these physically based models can be regarded as an equivalent steady-state runoff rate for soil erosion prediction purposes.

In WEPP, a soil erodibility parameter was introduced as a coefficient in the expression for the detachment capacity (Foster et al., 1995), while in GUEST, a different erodibility parameter was used as an exponent relating the sediment concentration at the transport limit to the actual sediment concentration (Rose, 1993). In both cases, data on runoff rate and sediment concentration are needed to evaluate soil erodibility parameters. Extensive experiments using rainfall simulators were undertaken for rangeland and cropland soils in the continental United States to determine soil erodibility for WEPP applications (Laflen et al., 1991a). To evaluate erodibility for tropical and sub-tropical soils in relation to GUEST development, rainfall and runoff rates during natural storm events were measured (Ciesiolka et al., 1995a). Apart from a few experimental sites, data on runoff rates are not routinely available by

Article was submitted for publication in June 1997; reviewed and approved for publication by the Soil & Water Div. of ASAE in March 1998.

The authors are **Bofu Yu, Uldis Cakurs,** and **Calvin W. Rose,** Faculty of Environmental Sciences, Griffith University, Nathan, Queensland, Australia. **Corresponding author:** Bofu Yu, Faculty of Environmental Sciences, Griffith University, Nathan, Queensland 4111, Australia; tel.: 617-3875-5258; fax: 617-3875-7459; e-mail: b.yu@ens.gu.edu.au.

comparison with event-based total runoff and soil loss amounts. This lack of runoff rate data has so far hindered the evaluation of soil erodibility parameters and the application of all process-based soil erosion models, not only the two mentioned above.

As observed by Stocking (1995), runoff and soil loss plots have been established at agricultural research stations in most countries in the world to measure the runoff amount and total soil loss to evaluate the effectiveness of various conservation technologies and management practices. In such experiments, eroded sediment and runoff were collected in a set of storage tanks mounted near the downslope end of the plots. Usually meteorological data such as rainfall rates are also available at or near these sites. If runoff rates can be reliably estimated using this widely available data on rainfall rates and total runoff amount, erodibility parameters could then be evaluated for soils in a wide range of climatic and physiographical environments, and the database for soil erodibility substantially expanded. Thus the ability to estimate runoff rates when rainfall rates and total runoff amount are known would facilitate wide-spread application of process-based soil erosion models. It is the purpose of this article to evaluate the adequacy of alternative ways in which runoff rates can be estimated from runoff amount and rainfall rate and how accurate are the estimates.

This article tests three different models for actual infiltration rate to estimate runoff rate at plot scales, and compares the estimated runoff rates with observed runoff rates at six sites in Southeast Asia and Australia. Performance of individual infiltration models is assessed in terms of the discrepancy in peak runoff rate and the effective runoff rate (i.e., eq. 1), and in terms of overall model efficiencies. In all cases it is assumed that rainfall rate during an event and total runoff for the event are measured.

DATA

Data on rainfall rates and runoff rates were collected using tipping buckets and data loggers from bare fallow plots at six sites in tropical and sub-tropical regions of Southeast Asia and Australia. The location, climate, soil characteristics, plot dimension, and slope were described elsewhere (Yu et al., 1997a) and their summary is presented in table 1. Experimental methodology and data management systems were described by Ciesiolka et al. (1995a). Descriptions of the sites with respect to various treatments were given for individual countries: Australia (Ciesiolka et al., 1995b), Malaysia (Hashim et al., 1995), the Philippines (Paningbatan et al., 1995; Presbitero et al., 1995). Bare plots were maintained using hand hoes at most sites. Weeds were controlled chemically at the Australian sites. No further disturbance of these bare plots has occurred after the commencement of these experiments. The 30 largest storm events in terms of rainfall amount for each site were used to test the performance of three simple infiltration models to estimate the runoff rates. Table 2 shows the average and standard deviation of rainfall amount, duration, peak rainfall rate, runoff amount, and peak runoff rate for each of the six sites. Both rainfall and runoff rates were measured at 1 min intervals. Since rainfall intensity at other sites may be recorded at time intervals other than 1 min, the original 1 min data were also accumulated at 6 min and 15 min intervals so that the model performance for different time intervals can be evaluated. These two multi-minute time intervals were selected because they are commonly used for storing historical rainfall intensity data. For example, Australian Bureau of Meteorology has adopted 6 min as the minimum time interval at which rainfall data can be supplied. The standard interval for rainfall intensity data is 15 min for the National Weather Service in the United States.

INFILTRATION MODELS AND METHOD OF ANALYSIS

For a given runoff plot, water balance for time interval i can be written as:

$$q_i = r_i - f_i - e_i - \frac{\Delta S_i}{\Delta t} \qquad (2)$$

Table 1. Bare plot characteristics at the six sites in Southeast Asia and Australia (adapted from Yu et al., 1997a)

Site	Country	Location	Soil Texture	MAR* (mm)	Area (m^2)	Length (m)	Slope† (%)
Goomboorian	Australia	26°04′S, 152°48′E	Sand	1 200	108	36	5
Imbil	Australia	26°26′S, 152°41′E	Loam	1 200	39	12.2	33
Kemaman	Malaysia	4°18′N, 103°19′E	Sandy loam	3 500	20	5	17
Los Baños	Philippines	14°6′N, 121°12′E	Clay	1 900	72	12	26
VISCA	Philippines	10°45′N, 124°49′E	Clay	2 200	71.4	11.9	50
Nan	Thailand	19°24′N, 100°45′E	Clay	1 200	216	36	Variable 12-50

* MAR = Mean annual rainfall.

† Each plot, though at different slope, was very approximately planar, but with unsurveyed natural irregularities in the 36 m length of plot.

Table 2. Summary statistics (average ± standard deviation) of the 1-min data for the 30 selected runoff events at these six sites in Southeast Asia and Australia

Site	Rainfall Amount (mm)	Peak Rainfall Rate (mm/h)	Event Duration (h)	Runoff Amount (mm)	Peak Runoff Rate (mm/h)	Effective Runoff Rate (mm/h)
Goomboorian	32.5 ± 30.6	76.9 ± 41.7	6.1 ± 5.6	15.4 ± 16.6	58.8 ± 45.0	25.9 ± 22.2
Imbil	86.1 ± 90.6	89.7 ± 50.9	14.8 ± 11.2	39.5 ± 62.5	53.3 ± 78.6	16.7 ± 25.6
Kemaman	54.0 ± 53.8	104.6 ± 34.2	4.7 ± 3.3	38.1 ± 49.2	84.9 ± 34.2	32.6 ± 14.7
Los Baños	50.4 ± 25.0	82.1 ± 38.2	8.0 ± 6.3	13.9 ± 11.1	34.7 ± 29.7	13.1 ± 11.1
VISCA	69.2 ± 64.8	100.8 ± 35.5	7.2 ± 5.8	4.0 ± 7.8	9.7 ± 8.0	2.9 ± 2.3
Nan	26.0 ± 22.0	69.0 ± 38.0	4.1 ± 3.3	3.8 ± 5.0	15.8 ± 20.1	8.0 ± 10.6

where r_i, f_i, and e_i are average rainfall, infiltration, and evaporation rates for the time interval, respectively; q_i is the average runoff rate at the plot exit; ΔS_i is the change in storage during the time interval Δt. Evaporation is neglible during a runoff event. The storage term in equation 2 can be ignored when the time interval is large relative to the hydrologic lag of the plot. As data are accumulated at large time intervals, the storage effect decreases and the difference between rainfall intensity and actual infiltration rate becomes an increasingly accurate estimate of the runoff rate at the plot outlet. Under these simplified conditions, runoff rate estimation can be reduced to determining actual rate of infiltration for the plot, f_i, in mm/h for each time interval of the event, so that the runoff rate at the plot scale can be estimated by:

$$q_i = r_i - f_i \tag{3}$$

where r_i is the rainfall rate in mm/h. The unknown rate of infiltration is subjected to the following two constraints:

$$\sum_{i=1}^{n} (r_i - f_i)\Delta t = Q_t \tag{4}$$

and

$$f_i \le r_i \tag{5}$$

where Q_t is the total runoff depth in mm for the event, Δt in hours is the time interval at which rainfall rate is measured, and $n\Delta t$ the duration of the runoff event. Equation 4 and inequality (eq. 5) place considerable constraints on the actual rate of infiltration. When modeling this actual rate of infiltration, these constraints will manifest themselves in terms of admissible model structures that the model could possibly assume, and likely parameter values for each model. In particular, if the infiltration model has only one parameter, its value can be uniquely determined by solving equation 4. Unlike most hydrologic modeling attempts whereby runoff or streamflow data are used to calibrate the model and to estimate model parameters, the approach adopted in this article involves identifying and assessing those simple models that do not require model calibration and parameter estimation using observed hydrographs. Observed runoff rates were used not to estimate the single parameter involved, but only to quantify the errors and model performances that are likely to occur at sites where runoff rate has not been measured. Advantages and disadvantages of this approach will be discussed later.

For this article, three simple infiltration models, each requiring only one parameter, are considered. The single parameter involved in each of the three models is determined in the program GOSH (Generation Of Synthetic Hydrographs) (Yu, 1997). Program GOSH calculates the unique value of the single parameter in each of three models, and uses this parameter to predict runoff rate as a function of time from measured rainfall rate and total event runoff. Thus, as the program name implies, a synthetic hydrograph is generated.

Model I - Constant Infiltration Rate

This constant infiltration rate is also known as ϕ-index (Chow et al., 1988; Linsley et al., 1988). In this model the actual infiltration rate is determined as:

$$f_i = \begin{cases} r_i & \text{if } r_i \le \phi \\ \phi & \text{otherwise} \end{cases} \tag{6}$$

No runoff would occur when the rainfall rate is less than the maximum rate of infiltration, ϕ. The maximum rate of infiltration is reached only when the rainfall rate exceeds the threshold and this threshold does not change over time within a runoff event and is applicable to the entire runoff plot. Model I can be regarded as a first-order approximation of the classical exponential decay in the rate of infiltration over time with a constant infiltration rate.

Model II - Constant Runoff Coefficient

It is assumed that the actual infiltration rate is proportional to the rainfall rate, i.e.:

$$f_i = (1 - R_c)r_i \tag{7}$$

where R_c is the runoff coefficient, which can easily be determined by:

$$R_c = \frac{Q_t}{P_t} \tag{8}$$

where P_t is the total rainfall depth (mm). The estimated runoff rate, $\hat{q}_i$, is simply given by:

$$\hat{q}_i = R_c r_i \tag{9}$$

These two models described above, especially the ϕ-index method are commonly found in hydrology text books (Chow et al., 1988; Linsley et al., 1988; Singh, 1992). Determination of the runoff coefficient is straightforward using equation 8 when the runoff depth is known. Calculation of the ϕ-index requires trial-and-error; its value is chosen such that the total rainfall depth above this threshold and runoff depth are equal (e.g., Chow et al., 1988). These two models are also known as constant loss rate model and proportional loss model, respectively, and they are widely used in engineering hydrology for flood estimation (Pilgrim and Cordery, 1993).

Model III - Variable Infiltration Rate

An infiltration parameter, I (in mm/h), is used to characterize the magnitude as well as the spatial variation of the maximum rate of infiltration across the plot. In this model, spatial variation is described by an exponential type model, the actual rate of infiltration being given by:

$$f_i = I\left(1 - e^{-r_i/I}\right) \tag{10}$$

The parameter, I, in this model can be interpreted as a spatially-averaged maximum infiltration rate. Equation 10 can be derived analytically assuming that the spatial

variation of the maximum rate of infiltration follows an exponential distribution with a mean of I (Hawkins and Cundy, 1987; Yu et al., 1997a). Model III can be regarded as a simplified version of the runoff routing model (Yu et al., 1997a) for runoff hydrographs at the plot scale. In Model III, initial amount of infiltration before runoff begins is not considered separately. The storage effect due to surface detention is also ignored.

The average maximum rate of infiltration, I, of Model III can be determined by substituting f_i in equation 4 with equation 10:

$$\sum_{i=1}^{n} \left[r_i - I\left(1 - e^{-r_i/I}\right) \right] \Delta t - Q_t = 0 \qquad (11)$$

and equation 11 can then be solved numerically for I when both rainfall rates, r_i, and runoff total, Q_t, are known. This is essentially a one-dimensional root-finding problem, and efficient and robust numerical methods are widely available. Brent's method which combines bisection and inverse quadratic interpolation (Brent, 1973; also Press et al., 1992) was used in program GOSH (Yu, 1997) to compute the parameter I. The ϕ-index in Model I was similarly computed, and there was really no need to use the tedious trial-and-error method commonly recommended (e.g., Chow et al., 1988).

Figure 1 shows the relationship between rainfall rate and actual infiltration rate for these three models. Only the shape of the various curves are important here because parameter values for these models were arbitrarily chosen. The critical difference between the first model with a constant infiltration rate and the other two is that the runoff duration is identical with rainfall duration for the latter two models, albeit the runoff rate can be extremely low when the rainfall rate is low for the variable infiltration rate model. For both constant infiltration rate and constant runoff coefficient models, the relationship between rainfall rate and runoff rate is linear, while the relationship is non-linear for the variable infiltration rate model.

To assess the various infiltration models for runoff rate estimation, the following five performance indicators were

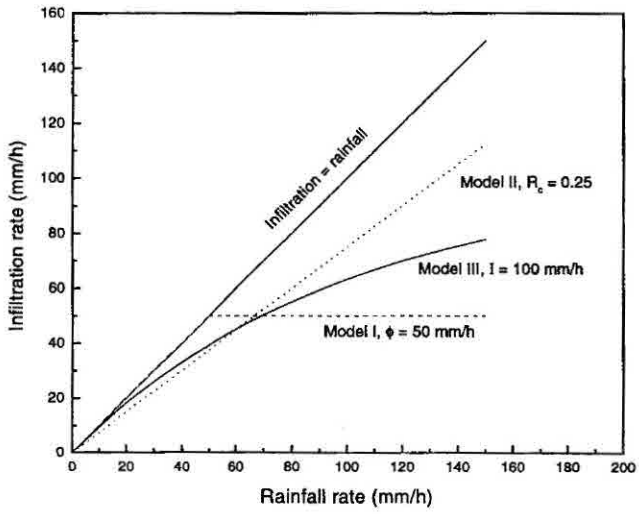

Figure 1–Relationship between actual rate of infiltration and rainfall rate for the three different infiltration models considered.

used: (1) relative error in the peak runoff rate; (2) relative error in the effective runoff rate; (3) the ratio of root mean square error (RMSE) in runoff rate to the peak runoff rate; (4) forecast efficiency, E_f; and (5) prediction efficiency, E_p. For relative errors, their frequency distribution is of particular interest because models producing bias should be avoided. The root mean square error for individual runoff events was calculated as:

$$\text{RMSE} = \sqrt{\frac{1}{n-1} \sum_{i=1}^{n} \left(\hat{q}_i - q_i\right)^2} \qquad (12)$$

and the ratio of RMSE to peak runoff rate quantifies the magnitude of the error in runoff rate relative to the magnitude of the runoff event. The forecast efficiency, E_f, for each hydrograph is defined as:

$$E_f = 1 - \frac{\sum \left(q_i - \hat{q}_i\right)^2}{\sum \left(q_i - \bar{q}\right)^2} \qquad (13)$$

where $\bar{q}$ is the average runoff rate for the event. This efficiency measure was proposed for use in hydrology by Nash and Sutcliffe (1970) and has since been widely used in hydrologic and soil sciences (Loague and Freeze, 1985; Risse et al., 1993; King et al., 1996). E_f indicates how close the scatter in a plot of observed versus estimated runoff rates are to the straight line at 45°. The efficiency measure can be less than zero, in which case model performance is no better than that using the known average runoff rate, i.e., Q_t/n.

Prediction efficiency, E_p, is calculated essentially in the same way as E_f except that observed and estimated runoff rates are sorted first before applying equation 13. It can be shown that prediction efficiency is always greater than forecast efficiency. Since the observed and estimated runoff rates are paired according to the ranks, prediction efficiency disregards any discrepancy in the timing of the runoff rates. Again, to use the scatter plot as an analogy, for E_f observed runoff rate is plotted against the estimated for each time interval, while for E_p, runoff rates are plotted for each rank. For identical measured and modeled hydrographs, both E_p and E_f would be one. If there is a time lag between the two otherwise identical hydrographs, E_f would decrease as the lag increases, while E_p would remain one. In essence, time lag between rainfall excess and runoff at the plot outlet due to the storage effect on the timing of peak runoff rate is discounted using the prediction efficiency.

The definition of E_f (eq. 13) is intended to be a general efficiency measure. q_i in equation 13 can be replaced by any other modeled quantities of interest. For example, the forecast efficiency for peak runoff rate, q_p, would be:

$$E_f \text{ for } q_p = 1 - \frac{\sum \left(q_p^{(j)} - \hat{q}_p^{(j)}\right)^2}{\sum \left(q_p^{(j)} - \bar{q}_p\right)^2} \qquad (14)$$

where $\bar{q}_p$ is the mean peak runoff rate and the superscript (j) indicates the event sequence number.

The five indicators described above quantify the model performance for individual runoff events. In addition, the forecast efficiency (eq. 14) was calculated for peak and effective runoff rates using results for all of the runoff events analyzed because these rates represent the most critical aspects of the hydrograph in the context of process-based soil erosion models.

RESULTS

Each of the three models was run for each of the 180 site-events and at each of three time intervals. The results are presented in two main sub-sections. First, results using 6 min data will be presented to show the best model for estimating the runoff rate. Secondly, errors in estimated runoff rate, in peak and effective runoff rates especially, using the best model available were assessed in relation to the magnitude of the runoff event and the time interval at which rainfall rate data were collected. Error assessment is an important part of model development and evaluation because guidelines on the quality of model output are needed for sites where runoff rate data are not available.

MODEL ASSESSMENT

Peak and effective runoff rates are the most important hydrologic variables in soil erosion models such as WEPP (Lane and Nearing, 1995) and GUEST (Misra and Rose, 1996). Figure 2 shows the frequency distribution of the relative error in peak runoff rate estimated using the three different infiltration models using 6 min rainfall and runoff data. Model I can be eliminated immediately because the magnitude of the relative error is considerably larger than that for other two models (fig. 2a). Sixty-one out of the 180 site events (34%) showed a relative error in excess of 100%. The fact that the model tends to overestimate the peak runoff rate suggests that the actual rate of infiltration when the peak rainfall rate occurred was much higher than the constant rate of infiltration determined for the model. The difference between Model II and Model III are not great in terms of the magnitude of the relative error in peak runoff rate (figs. 2b, 2c, and also table 3). Model II, however, has systematically underestimated the peak runoff rate (fig. 2b). The mode of the frequency distribution for Model II is between –30 and –40%, and for 92% of the site events the error was negative. By contrast, the relative error in peak runoff rate using Model III is almost symmetrically distributed around zero with 35% of site events in the range from –10% to 10% and 56% of site events from –20% to 20% (fig. 2c), although large relative error can occur when the runoff rate is small. For example, for the 10 events with a relative error in excess of 100% using Model III, the mean runoff amount and peak runoff rate were only 12.1 mm and 6.2 mm/h, respectively. For small runoff events with low runoff rate, the relative error in the data on rainfall and runoff rates can be quite large (Yu et al., 1997b). Whether or not an infiltration model introduces any bias in estimated runoff rate is an important consideration because bias cannot be removed by averaging. As long as there is no bias, errors in soil erodibility parameters determined using the estimated peak runoff rate can be reduced by averaging the results from a number of runoff events. Frequency distribution of the relative error in the effective runoff rate shows a similar pattern for the three models. Considering both the magnitude and frequency distribution of the errors in the peak runoff rate, model III is clearly superior to the other two infiltration models.

The median performance of all three models in terms of all five indicators is summarized in table 3. It can be seen that errors are large and model efficiencies are low for Model I. The primary difference between Model II and Model III is that Model II underestimates both peak runoff

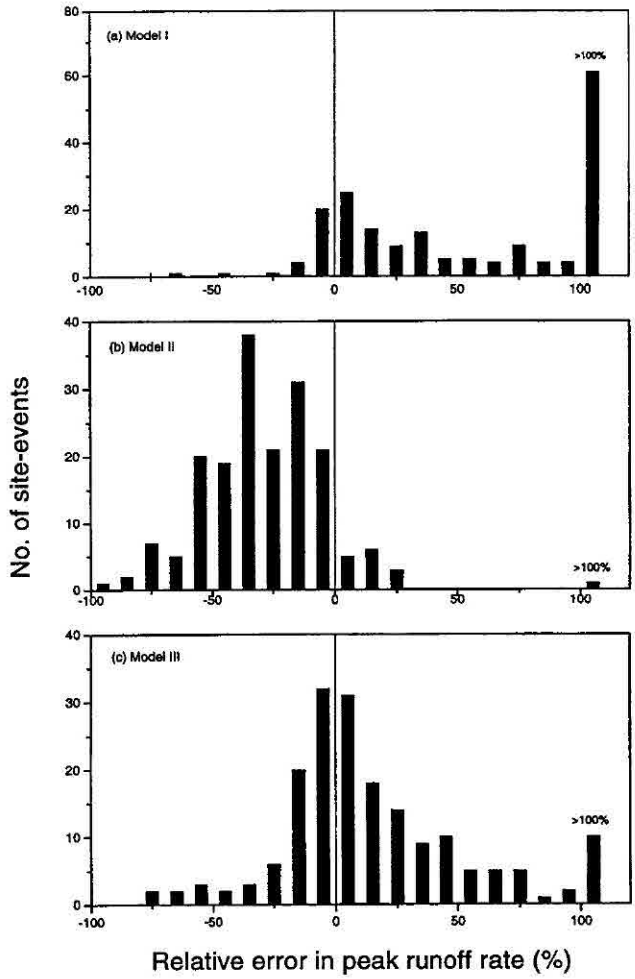

Figure 2–Frequency distribution of the relative error in peak runoff rate in terms of number of site-events out of 180 using the three infiltration models: (a) Model I with a constant rate of infiltration; (b) Model II with an infiltration rate in proportion to the rainfall rate; and (c) Model III with a spatially variable rate of infiltration.

Table 3. Median performance of the three infiltration models using 6 min data and of Model III with a variable infiltration rate at different time intervals

Model	Time Interval (min)	Error in q_p (%)	Error in q_e (%)	RMSE/q_p (%)	E_f for Hydro-graph	E_p for Hydro-graph	E_f for q_p	E_f for q_e
I	6	45	89	21	–0.13	0.67	0.84	0.55
II	6	–31	–35	12	0.61	0.86	0.86	0.81
III	1	14	13	13	0.13	0.89	0.83	0.89
III	6	6	8	13	0.52	0.92	0.94	0.93
III	15	10	7	13	0.73	0.92	0.93	0.94

* Forecast efficiency for peak and effective runoff rate based on all of the 180 site-events is also included.

rate and the effective runoff rate, and has a lower prediction efficiency as well.

In table 3, the performance of Model III at different time intervals is also presented. The variation in the model performance at different time intervals is small in terms of the relative error or prediction efficiency. The trend, if any, in the model performance is that Model III tends to work better according to these indicators at larger time intervals. This is probably because the relative error in the rainfall and runoff data decreases as the time interval increases (Yu et al., 1997b), and as a result, the data used for model assessment is of higher quality at larger time intervals. Of particular interest is the significant increase in the forecast efficiency as the time interval increases (table 3). As noted previously, forecast efficiency is a more stringent test of the goodness of fit because both the magnitude and timing of the runoff rate have to be right to achieve a high forecast efficiency. As the time interval increases, the lag between rainfall excess and runoff at plot outlet becomes small relative to the time interval used for runoff measurement. The runoff rate estimated using equation 3 better approximates the actual runoff rate measured at the plot outlets. As a result, as time interval increases, the timing of estimated runoff rate improves, and concomitantly the forecast efficiency improves (table 3). The prediction efficiency on the other hand does not vary as much as time interval increases. For practical purposes, especially in the context of estimating soil erodibility parameters, the timing of runoff rate is of a lesser concern by comparison with the magnitude of the runoff rate. The prediction efficiency is therefore a better indicator of the model performance in this context.

Since Model III is just as simple as the other two models, but consistently out-performed the other two, and Model III works equally well for a range of time scales, we therefore recommend that Model III be used as a general one-parameter infiltration model for runoff rate estimation at the plot scale when runoff amount is known. Error assessment using only Model III will now be presented.

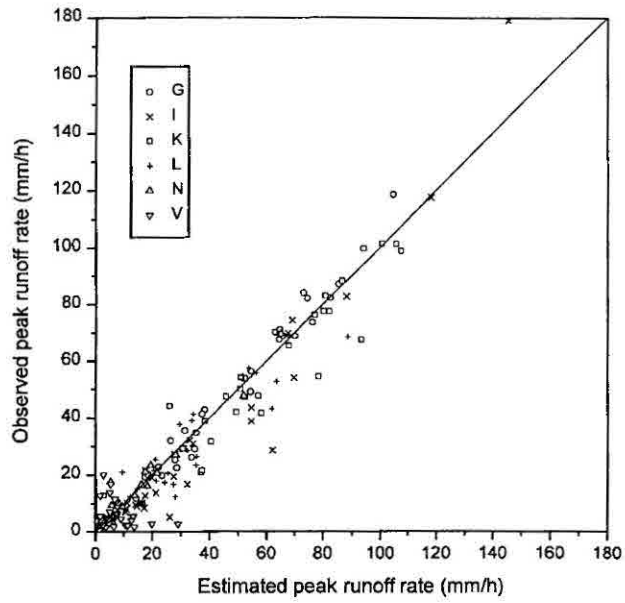

Figure 3–Estimated vs observed peak runoff rate using Model III for all the 180 site events using 6 min data. The characters in the legends stand for individual sites: G - Goomboorian; I - Imbil; K - Kemaman; L - Los Baños; N - Nan, and V - VISCA. The forecast efficiency is 0.94.

Table 4. Summary of the error in estimated peak and effective runoff rates at three time intervals

	1-min		6-min		15-min	
	q_p	q_e	q_p	q_e	q_p	q_e
Average observed (mm/h)	42.9	16.5	28.9	14.0	19.6	11.2
Average estimated (mm/h)	47.5	18.6	30.6	15.4	20.6	12.1
Relative bias (%)	11	12	6	10	5.3	7.6
Mean AE* (mm/h)	10.8	3.9	4.6	2.5	3.5	1.8
Median AE* (mm/h)	6.1	2.0	2.3	1.2	2.1	0.8
90% of AE* less than (mm/h)	24.5	10.0	11.4	6.9	8.0	5.3

* AE = absolute error.

Error Assessment

In each of the three infiltration models the single parameter involved is uniquely determined, essentially by satisfying mass conservation of water. Thus, apart from data errors, there is no error in the single parameter employed. However, even though each model satisfies mass conservation of water for the event as a whole, there will be error in infiltration and runoff rates predicted as a function of time within the event. This section addresses the vital question of error in the synthetic hydrograph predicted for sites where runoff rate was not measured. The error in the peak and effective runoff rate estimated from the synthetic hydrograph was examined for all 180 site events and for a range of time intervals. Figure 3 shows a scatter plot of the estimated against observed peak runoff rates using the 6 min data. It can be seen that the observed values cover a range of peak runoff rate up to 180 mm/h, and the overall fit is very good with a forecast efficiency of 0.94 (table 3). The forecast efficiency is high for individual sites as well. Three of the six sites have E_f in excess of 0.9. The lowest is 0.53 at VISCA. The model tends to over-estimate the peak runoff rate with a relative bias of 6% (table 4). The errors do not seem to increase with the peak runoff rate, suggesting that the relative error would decrease with peak runoff rate. The mean absolute error does not change greatly with peak runoff rate with a mean of 4.6 mm/h, or 16% of the average observed peak runoff rate. Figure 4 shows the corresponding scatter plot for the effective runoff rate. A similar pattern in the error can be noted. The mean absolute error is 2.5 mm/h for the effective runoff rate or 18% of the average observed peak runoff rate (table 4). In table 4, errors in estimated peak and effective runoff rates are summarized for all three time intervals used in the article. As the time interval increases by a factor of 15, the peak and effective runoff rates decrease by a factor of 2.2 and 1.5, respectively. At the same time, the mean absolute error also decreases by a factor of 2.9 for peak runoff rate and 2.1 for effective runoff rate. The fact that the errors decrease faster than the runoff rates as the time interval is increased and the trends of decreasing bias and increasing forecast efficiency all show that there is improvement in model performance as the time interval is increased. As noted before, this improvement may be related to a reduced relative error in the rainfall and runoff data.

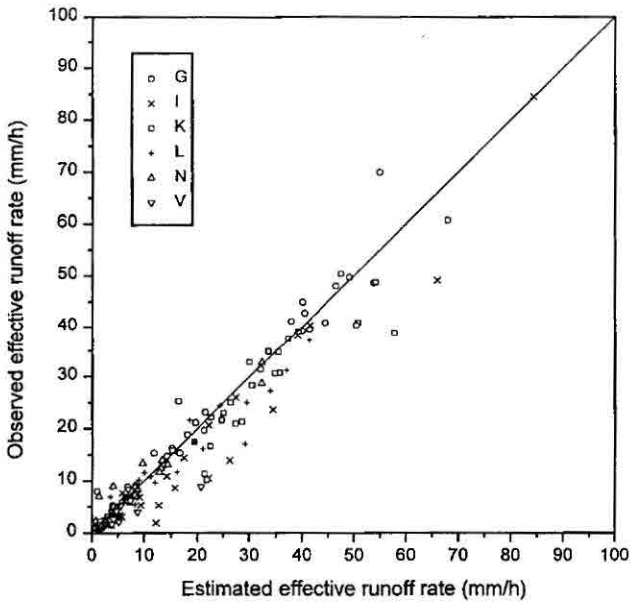

Figure 4–Estimated vs observed effective runoff rate for all the 180 site events using 6 min data. The characters in the legends stand for individual sites: G - Goomboorian; I - Imbil; K - Kemaman; L - Los Baan; L - Los Baños; N - Nan, and V - VISCA. The forecast efficiency is 0.93.

The ratio of root mean square error (RMSE) to peak runoff rate is a different measure of the error magnitude to those presented in table 4. First, this ratio is always positive. Secondly, the ratio can be interpreted as a noise to signal ratio. Graphically, the ratio represents the average size of the error bar relative to the height of the hydrograph. This ratio therefore characterizes the relative error for the hydrograph as a whole as distinct from the relative error in peak or effective runoff rate, and as such should be related to runoff amount or runoff coefficient for the event. Figure 5 shows a scatter plot of the runoff coefficient versus the ratio of RMSE to peak runoff rate using 6 min data for all 180 site events. It can be seen that this ratio tends to decrease as the runoff coefficient increases. Straight lines are drawn to separate 18 site events from the rest of the graph, and these lines approximately define the 90% interval for the RMSE to peak runoff rate ratio. The equations for the 90% confidence interval are:

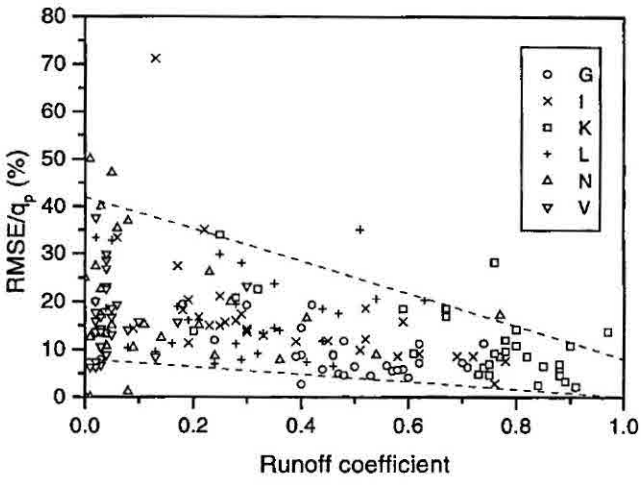

Figure 5–The relationship between the runoff coefficient and the relative error in terms of the root mean square error as percent of the peak runoff rate for all the 180 site events. The characters in the legends stand for individual sites: G - Goomboorian; I - Imbil; K - Kemaman; L - Los Baños; N - Nan, and V - VISCA. The dashed lines (eq. 15) represent the 90% confidence interval for the relative error.

$$\text{Upper limit:} \quad RMSE/q_p\,(\%) = 43(1 - 0.81\,R_c)$$

$$\text{Lower limit:} \quad RMSE/q_p\,(\%) = 8(1 - R_c) \qquad (15)$$

At R_c = 0.1, the 90% confidence interval for the noise to signal ratio is 7.2 to 40%, and at R_c = 0.9, the confidence interval is reduced to 0.8 to 12%. The relationship between the relative error and runoff coefficient is essentially the same for the other two time intervals. The error magnitude for peak and effective runoff rates, and equation 15 for the ratio of the root mean square error to peak runoff rate can be coded in computer programs as a guide to the likely errors in the estimated runoff rate using Model III with an infiltration rate variable with rainfall rate.

Further Validation of Model III Using Experimental Results

In most experimental studies of infiltration and runoff at the plot scale using rainfall simulators, a uniform rainfall intensity is usually applied and then a decrease of the infiltration rate over time is always observed, although during natural storm events rainfall intensity always shows considerable temporal variation. Of the few experiments that simulate storm patterns with varying rainfall intensity, Flanagan et al. (1988) investigated the effects of storm pattern on runoff and infiltration. They used a programmable rainfall simulator to generate 1 h storms with a single peak in rainfall intensity. The plot size was 3.0 m wide and 9.9 m long with an average slope of 6.8%. In addition to a uniform storm of 64 mm/h (UN), five storm patterns of variable intensity were used. Four patterns peaked at 250 mm/h with peaks occurring at 0 min (FQ), 20 min (SQ), 40 min (TQ), and 60 min (LQ) into the 1 h runs. The sixth pattern was generated with a peak intensity of 125 mm/h at 20 min (SS). Of the six storm patterns generated, three, i.e., SQ, TQ, and SS (Flanagan et al., 1988), were selected here to further test the infiltration models considered in this article because these were the only ones with zero rainfall intensity at the beginning and the end of the 1 h period, thus constituting a complete storm event comparable to those considered in this article. The artificial storm patterns represented at 1 min intervals and observed runoff amounts were used to

Table 5. A comparison of observed vs predicted peak runoff rates using experimental data from Flanagan et al. (1988)

Storm Pattern*	Total Rain* (mm)	Peak Rainfall Intensity* (mm/h)	Total Runoff* (mm)	Peak Runoff Rate* (mm/h)	Predicted Peak Runoff Rate (mm/h) Using GOSH Model I	Model II	Model III
SQ	63.3	250	1.1	13	38.5	4.3	8.6
TQ	63.3	250	2.2	19	56.2	8.7	17.1
SS	62.5	125	1.1	4	16.5	2.2	3.3

* Data from Flanagan et al. (1988).

compute the peak runoff rate using program GOSH (Yu, 1997). Predicted and observed peak runoff rates are presented in table 5. It can be seen that Model III has produced by far the best results in terms of the predicted peak runoff rate. The percentage error in peak runoff rate using Model III varying from 10% to 34% are comparable to errors reported for the six field sites considering the low runoff coefficients of only 2% to 4% for these experiments.

DISCUSSION

This article has demonstrated that a one-parameter infiltration model can be used to estimate the runoff rates at the plot scale when rainfall rates and total runoff amount are known. The best model for the extensive data sets employed has been shown to be the one that takes into account the spatial variation of the maximum rate of infiltration over the runoff plot. Selecting parameter values, necessary for more complicated hydrologic models, is no longer an issue for one-parameter models because the parameter values are uniquely determined through water balance for the runoff event. There is little doubt that model performance would improve if more parameters and more complicated model structures are introduced, although whether or not using such complicated models are worth the effort is debatable. At least two arguments can be made against using more complicated models. First, the improvement, if any, in model performance would be marginal given the high prediction efficiency that has been achieved at a range of time scales (table 3). Secondly, to use more complicated models, one has to know the parameter values for sites where data on runoff rate have not been collected because when there is more than one parameter, model parameters cannot be determined using runoff totals alone.

All the models considered in this article disregard any decrease in the rate of infiltration over time. In Model II and Model III, which outperformed Model I using both field and experiment data, actual infiltration rate has been assumed to be a function of rainfall rate only. This dependence of actual infiltration rate on rainfall intensity suggests a considerable spatial variation in the rate of infiltration. As early as 1946, Cook (1946) noted a dependence of infiltration rate on rainfall intensity. Moldenhauer et al. (1960), Murai and Iwasaki (1975), Hawkins (1982), and Flanagan et al. (1988) also found that infiltration rate increases as rainfall intensity increases and attributed this positive relationship to spatial variability in the maximum infiltration rate across the field. Model III considered in this article represents the simplest possible formulation of this spatial variability. The parameter I quantifies both the magnitude of the infiltration rate and its spatial variability. The classic exponential decay in infiltration rates over time holds and is readily observable when a constant rainfall intensity is applied. During natural rainfall events, however, rainfall intensity rarely if ever, remains constant for any significant amount of time. The highly variable nature of rainfall intensity during real storm events is such that spatial variability of infiltration rate features more prominently than the decrease in time of the infiltration rate at a point in the landscape.

Although the 180 runoff events considered in this article cover a wide range of hydrologic conditions in terms of the runoff coefficient (fig. 5), rainfall rate and total amount (table 2), most of the experimental plots have steep slopes (> 10% at five of the six sites). Being bare, these plots do not have large interception and depression storage that can significantly reduce both runoff amount and peak runoff rate. The applicability of this simple model may be limited to situations where runoff is more responsive to rainfall. Given that soil loss is most severe on steep slopes with poor vegetative cover and during large rainfall events and soil erodibility is routinely determined using runoff and soil loss data from bare fallow plots, this simple infiltration model works best when water-related soil erosion matters most. The model recommended in this article is therefore of relevance in the context of soil erosion research in general and estimating soil erodibility parameters in particular.

CONCLUSION

Three one-parameter infiltration models were evaluated to meet the need for estimating runoff rates at the plot scale when total runoff amount and rainfall rates are known. It is found that the model that takes into account the spatial variation of the infiltration rate works better than the traditional constant infiltration rate or proportional infiltration rate models. This simple infiltration model assuming a spatial variable rate of infiltration has the distinct advantage of not requiring parameter estimation at sites with event runoff data and works equally well using rainfall data collected at a range of time intervals. The model has minimum bias with respect to peak and effective runoff rate. At a typical time interval of 6 min, the relative bias of the estimated peak runoff rate is 6% and the mean absolute error is 4.6 mm/h, while the relative bias of the estimated effective runoff rate and the mean absolute error are 10% and is 2.5 mm/h, respectively. The ratio of root mean square error to peak runoff rate was found to decrease as runoff coefficient increases.

ACKNOWLEDGMENT. We acknowledge the financial support from the Australian Centre for International Agricultural Research for the project 'Validation and Application of Physically-based Soil Erosion Model at IBSRAM-ASIALAND sites'. We thank all of those involved in the experiment design and set-up, data collection and management for the project, especially C. A. A. Ciesiolka (Queensland Department of Primary Industries), S. M. Hashim (Malaysian Agricultural Research and Developmental Institute), E. P. Paningbatan, Jr. (University of the Philippines at Los Baños), and Mr. C. Anecksamphant and his team (Department of Land Development, Thailand). We also thank anonymous reviewers for their many constructive comments. They have brought our attention to the experimental work by Flanagan et al. (1988).

REFERENCES

Brent, R. P. 1973. *Algorithms for Minimization Without Derivatives*. Englewood Cliffs, N.J.: Prentice-Hall.

Chow, V. T., D. R. Maidment, and L. W. Mays. 1988. *Applied Hydrology*. New York, N.Y.: McGraw-Hill.

Ciesiolka, C. A. A., K. J. Coughlan, C. W. Rose, M. C. Escalante, G. M. Hashim, E. P. Paningbatin Jr., and S. Sombatpanit. 1995a. Methodology for a multi-country study of soil erosion management. *Soil Technol.* 8(3):179-192.

Ciesiolka, C. A. A., K. J. Coughlan, C. W. Rose, and G. D. Smith. 1995b. Erosion and hydrology of steeplands under commercial pine apple production. *Soil Technol.* 8(3):243-258.

Cook, H. L. 1946. The infiltration approach to the calculation of surface runoff. *Eos Trans. AGU* 27:726-747.

Flanagan, D. C., G. R. Foster, and W. C. Moldenhauer. 1988. Storm pattern effect on infiltration, runoff, and erosion, *Transactions of the ASAE* 31(2):414-420.

Foster, G. R., D. C. Flanagan, M. A. Nearing, L. J. Lane, L. M. Risse, and S. C. Finkner. 1995. Hillslope Erosion Component, Ch. 11. In *USDA Water Erosion Prediction Project: Hillslope Profile Model Documentation*, NSERL Report No. 2, eds. L. J. Lane and M. A. Nearing. West Lafayette, Ind.: National Soil Erosion Laboratory, USDA-ARS.

Hawkins, R. H. 1982. Interpretation of source-area variability in rainfall-runoff relationships. In *Rainfall- Runoff Relationships*, 303-324, ed. V. P. Singh. Fort Collins, Colo: Water Resources Publications.

Hawkins, R. H., and T. W. Cundy. 1987. Steady-state analysis of infiltration and overland flow for spatially-varied hillslopes. *Water Resour. Bull.* 23(2):251-256.

Hashim, G. M., C. A. A. Ciesiolka, W. A. Yusoff, A. W. Nafis, M. R. Mispan, C. W. Rose, and K. J. Coughlan. 1995. Soil erosion processes in sloping land in the east coast of Peninsular Malaysia. *Soil Technol.* 8(3):215-233.

King, K. W., C. W. Richardson, and J. R. Williams. 1996. Simulation of sediment and nitrate loss on a vertisol with conservation tillage practices. *Transactions of the ASAE* 39(1):34-38.

Laflen, J. M., W. J. Elliot, J. R. Simanton, C. S. Hollzhey, and K. D. Kohl. 1991a. WEPP soil erodibility experiments for rangeland and cropland soils. *J. Soil & Water Conservation* 46(1):39-44.

Laflen, J. M., L. J. Lane, and G. R. Foster. 1991b. WEPP: A new generation of erosion prediction technology. *J. Soil & Water Conservation* 46(1):34-38.

Lane, L. J., and M. A. Nearing, eds. 1995. USDA Water Erosion Prediction Project: Hillslope Profile Model Documentation. NSERL Report No. 2. W. Lafayette, Ind.: National Soil Erosion Laboratory, USDA-ARS.

Linsley, R. K., M. A. Kohler, and J. H. Paulhus. 1988. *Hydrology for Engineers*. New York, N.Y.: McGraw-Hill,

Loague, K. M., and R. A. Freeze. 1985. A comparison of rainfall-runoff modelling techniques on small upland catchments. *Water Resour. Res.* 21(2):229-248.

Misra, R. K., and C. W. Rose. 1996. Application and sensitivity analysis of process-based erosion model GUEST. *European J. Soil Sci.* 47(4):593-604.

Moldenhauer, W. C., W. C. Burrows, and D. Swartzendruber. 1960. Influence of rainfall storm characteristics on infiltration measurements, *7th Int. Congr. Soil Sci.* 1:426-432.

Murai, H., and Y. Iwasaki. 1975. Studies on function of water and soil conservation based on forest land (I) - Influence of difference in forest condition upon water run-off, infiltration and erosion, 23-84. Bulletin No. 274. Tokyo, Japan: The Govn. Forest Exp. Sta.

Nash, J. E., and J. V. Sutcliffe. 1970. River flow forecasting through conceptual models, Part 1: A discussion of principles. *J. Hydrol.* 10(3):282-290.

Oldeman, L. R., R. T. A. Hekkeling, and W. G. Sombroek. 1991. World map of the status of human-induced soil degradation: An explanatory note. Wageningen, the Netherlands: International Soil Reference and Information Centre.

Paningbatan Jr., E. P., C. A. A. Ciesiolka, K. J. Coughlan, and C. W. Rose. 1995. Alley cropping for managing soil erosion of hilly lands int the Philippines. *Soil Technol.* 8(3):193-204.

Pilgrim, D. H., and I. Cordery. 1993. Flood Runoff, Ch. 9. In *Handbook of Hydrology*, ed. D. R. Maidment, 9.1-9.41. New York, N.Y.: McGraw-Hill.

Presbitero, A. L., M. C. Escalante, C. W. Rose, K. J. Coughlan, and C. A. A. Ciesiolka. 1995. Erodibility evaluation and the effect of land management practices on soil erosion from steep slopes in Leyte, the Philippines. *Soil Technol.* 8(3):205-213.

Press, W. H., B. P. Flannery, S. A. Teukolsky, and W. T. Vetterling. 1992. *Numerical Recipes: The Art of Scientific Computing*. Cambridge, U.K.: Cambridge University Press.

Renard, K. G., G. R. Foster, G. A. Weesies, D. K. McCool, and D. C. Yoder. 1997. *A Guide to Conservation Planning with the Revised Universal Soil Loss Equation (RULSE)*. Agriculture Handbook No. 703. Washington, D.C.: USDA.

Risse, L. M., M. A. Nearing, A. D. Nicks, and J. M. Laflen. 1993. Error assessment in the Universal Soil Loss Equation. *Soil Science Soc. Am. J.* 57(3):825-833.

Rose, C. W. 1993. Erosion and sedimentation. In *Hydrology and Water Management in the Humid Tropics*, eds., M. Bonell, M. M. Hufschmidt, and J. S. Gladwell, 301-343. Cambridge, U.K.: Cambridge University Press.

Rose, C. W. 1994. Research progress on soil erosion processes and a basis for soil conservation practices. In *Soil Erosion Research Methods*, ed. R. Lal, 159-178. Defray Beach, Fla.: Soil and Water Conservation Society, St Lucie Press.

Singh, V. P. 1992. *Elementary Hydrology*. Englewood Cliffs, N.J.: Prentice Hall.

Stocking, M. 1995. Soil erosion and land degradation. In *Environmental Science for Environmental Management*, ed. T. O'Riordan. London, England: Longman Scientific & Technical.

Wischmeier, W. H., and D. D. Smith. 1978. *Predicting Rainfall Erosion Losses—A Guide to Conservation Planning*. Agriculture Handbook No. 537. Washington, D.C.: USDA.

Yu, B. 1997. GOSH: A program for calculating runoff rates given rainfall rates and runoff amount, User guide and reference manual. ENS Working Paper, 2/97. Nathan, Queensland, Australia: Faculty of Environmental Sciences, Griffith University.

Yu, B., C. W. Rose, K. J. Coughlan, and B. Fentie. 1997a. Plot-scale rainfall-runoff characteristics and modeling at six sites in Australia and Southeast Asia. *Transactions of the ASAE* 40(5):1295-1303.

Yu, B., C. A. A. Ciesiolka, C. W. Rose, and K. J. Coughlan. 1997b. A note on sampling errors in the rainfall and runoff data collected using tipping bucket technology. *Transactions of the ASAE* 40(5):1305-1309.